Available online at www.sciencedirect.com
SCIENCE DIRECT®
Forest Ecology and Management 198 (2004) 149–167
Forest Ecology and Management
www.elsevier.com/locate/foreco

Relationships between forest stand parameters and Landsat TM spectral responses in the Brazilian Amazon Basin

Dengsheng Lu[a,*], Paul Mausel[b], Eduardo Brondízio[c], Emilio Moran[a,c]

[a]*Center for the Study of Institutions, Population, and Environmental Change (CIPEC), Indiana University, 408 N. Indiana Avenue, Bloomington, IN 47408, USA*
[b]*Department of Geography, Geology, and Anthropology, Indiana State University, Terre Haute, IN, USA*
[c]*Anthropological Center for Training and Research on Global Environmental Change (ACT), Indiana University, Bloomington, IN, USA*

Received 9 December 2003; received in revised form 23 February 2004; accepted 29 March 2004

Abstract

Estimation of forest stand parameters such as aboveground biomass in a large area using remotely sensed data has considerable significance for sustainable management and utility of natural resources. In practice, selecting suitable image data for such purposes remains difficult due to a poor understanding of forest stand parameters and remote-sensing spectral response relationships, particularly in moist tropical regions. This paper explores relationships between forest stand parameters and Landsat Thematic Mapper (TM) spectral responses through analyses of three study areas in the eastern Amazon basin (Altamira, Bragantina, and Ponta de Pedras). Six TM bands and many vegetation indices are examined through integration of spectral responses and field vegetation inventory data. Pearson's correlation coefficients are used to interpret relationships between forest stand parameters and TM data. This study concludes that single band TM5 and linear transformed indices such as PC1 (the first component in a principal component analysis), KT1 (brightness of the tasseled cap transform), and albedo are most strongly correlated with forest stand parameters, somewhat independent of biophysical environments. Many vegetation indices that use TM4 and TM3 data, such as the atmospherically resistant vegetation index, the atmospheric and soil vegetation index, and the normalized difference vegetation index, are weakly correlated with selected forest stand parameters. In contrast, vegetation indices using band TM5 data improve correlations with selected forest stand parameters in Altamira forests that are characterized by a complex stand structure. Forest stand structure and associated canopy shadow affect the forest stand parameters and TM spectral response relationships. This paper provides a better understanding of relationships that have a potential of being important for developing stand parameter estimation models and for improvement of vegetation classification accuracy.

Keywords: Forest stand parameters; Spectral responses; Vegetation index; Correlation; Moist tropical forest

1. Introduction

Forests are widely distributed on the Earth and are important natural resources for human survival. Sustainable management and utility of forest resources require accurate information about their extent and

* Corresponding author. Tel.: +1 812 856 3102; fax: +1 812 855 2634.
E-mail address: dlu@indiana.edu (D. Lu).

0378-1127/$ – see front matter © 2004 Elsevier B.V. All rights reserved.
doi:10.1016/j.foreco.2004.03.048

spatial distribution. Forest stand parameters, such as volume or biomass, average stand diameter and height, are important data needed to assess forest resources. Traditional inventory of forest stand parameters based on fieldwork is often difficult, costly, and time-consuming to conduct in a large area, particularly in moist tropical regions. Remote sensing may be the only feasible way to acquire forest stand parameter information at a reasonable cost, with acceptable accuracy, and feasible effort because of its data advantages which include repeated data collection, multispectral and multitemporal images, synoptic view, fast digital processing of large quantities of data, and compatibility with geographic information systems (GIS). Modern remote-sensing techniques, such as multi-sensor data fusion, increased spatial and spectral resolution, and integration of remote-sensing and GIS make remotely sensed data the primary source for many applications, such as land-use/land-cover classification, change detection, and estimation of forest stand parameters.

Recently, much remote-sensing research has focused on the extraction of forest stand parameters through correlation or regression analysis to examine relationships between spectral response and structural factors of coniferous forest, including basal area, biomass, crown closure, diameter at breast height (DBH), tree height, vegetation density, and leaf area index (LAI) using optical sensor data such as Landsat Thematic Mapper (TM) images (Franklin, 1986; Horler and Ahern, 1986; Peterson et al., 1986, 1987; Spanner et al., 1990; Stenback and Congalton, 1990; Lathrop and Pierce, 1991; Ardo, 1992; Curran et al., 1992; Cohen et al., 1995; Gemmell, 1995; Kimes et al., 1996; Trotter et al., 1997; Turner et al., 1999; Eklundh et al., 2001; Franco-Lopez et al., 2001). Similar forest parameter data have been acquired through analysis of microwave radar images such as synthetic aperture radar (SAR) (Israelsson et al., 1994; Rauste and Hame, 1994; Harrell et al., 1995, 1997; Fransson and Israelsson, 1999; Kurvonen et al., 1999; Santoro et al., 2001; Castel et al., 2002; Sun et al., 2002). Due to the important roles of moist tropical forests in global warming, biodiversity, and ecosystems, research using remotely sensed data to measure selected properties of tropical forest stand parameters has increasingly attracted interest during the past decade (Cook et al., 1989; Sader et al., 1989; Wu, 1990; Lucas et al., 1993; Foody and Curran, 1994; Nelson et al., 2000; Steininger, 2000; Lu, 2001; Tetuko et al., 2001; De Wasseige and Defourny, 2002; Drake et al., 2002; Lu et al., 2002a; Santos et al., 2002). Wulder (1998) summarizes many image processing methods that may be useful for estimation of forest structural parameters using remotely sensed data.

Although much remote-sensing research has been conducted during the past decades, conclusions about relationships between forest stand parameters and spectral responses vary, depending on the characteristics of the study areas. Identifying the spectral wavelengths or wavelength combinations that are most suitable to use to acquire information about a specific biophysical parameter in a given study area is difficult. The influence of different characteristics of study areas on these spectral-forest parameter relationships is poorly understood. This is especially true in moist tropical regions because of their complex forest stand structure and abundant vegetation species. Most previous research of this type was focused on the boreal or temperate forest due to their relatively simple stand structure and tree species. However, relatively less attention has been devoted to the moist tropical regions due to the difficulty in field data collection and the complex biophysical environments. A good understanding of forest stand parameters and remote-sensing spectral relationships is a prerequisite for effectively using appropriate image bands for developing forest stand parameter estimation models and for classifying vegetation classes. Hence, a comparative analysis of spectral responses and biophysical parameters in different forest stand structures and environmental conditions is needed to explore these relationships and to explore the effects of different characteristics of the study areas on them. For this purpose, three study areas in Altamira, Bragantina, and Ponta de Pedras in the eastern Amazon basin were selected, and field vegetation inventory data were collected. Six TM bands (excluding thermal band TM6 due to low spatial resolution) and a variety of vegetation indices were used in this research to identify the TM bands and vegetation indices that were most strongly correlated with the selected forest stand parameters in the Amazon basin, as well as to explore the impacts of forest stand structures on TM response and selected stand parameter relationships.

2. Previous work

2.1. TM spectral signature and forest stand parameter relationships

It is essential to establish correct relationships between forest cover and image data to understand how image data relate to forest stand characteristics (Franklin, 1986; Wulf et al., 1990; Lathrop and Pierce, 1991). Previous studies have shown that visible bands are strongly related to biomass (Franklin, 1986; Roy and Ravan, 1996; Jakubauskas and Price, 1997) and middle infrared bands have strongly negative relationships with stand timber volume (Ahern et al., 1991; Ripple et al., 1991; Ardo, 1992; Gemmell, 1995; Roy and Ravan, 1996). Many studies have identified middle infrared wavelengths as being most sensitive to change in forest wood volume, with reflectance in this region being directly related to the extent of canopy closure (Butera, 1986; Horler and Ahern, 1986). Steininger (2000) found a significant relationship between middle infrared reflectance and secondary forest aboveground biomass in Manaus, Brazil, but such significant relationships were not observed in Santa Cruz de la Sierra, Bolivia. A possible reason for these results in both study areas is the effects of a low sun angle during the satellite measurement in Bolivia and regrowth structural and general compositional differences between the two study areas. Eklundh et al. (2001) also found that middle infrared wavelengths, in particular, band 7 in ETM+, were significant related to LAI in a boreal conifer forest.

The correlation of forest stand parameters with near infrared wavelength reflectance may be positive (Spanner et al., 1990), negative (Ripple et al., 1991; Danson and Curran, 1993), or flat (Franklin, 1986; Peterson et al., 1987) because of increased canopy shadowing with larger stands and decreased understory brightness (soil brightness) due to increased density with biomass increase (Horler and Ahern, 1986; Spanner et al., 1990; Roy and Ravan, 1996; Treitz and Howarth, 1999). Shadowing probably plays an important part in the response of all bands to change in wood volume (Ardo, 1992) and it is thought to be at least as important as canopy water content in determining the middle infrared responses (Horler and Ahern, 1986). TM data may provide information on stand density but not on species composition (Horler and Ahern, 1986). Franklin (1986) found that sample plots grouped by species structure had a much better statistical relationship between forest attributes and TM reflectance data than by using species or structure alone.

2.2. Vegetation index and forest stand parameter relationships

A variety of vegetation indices have been developed, with the most popular ones using red and near infrared wavelengths to emphasize the difference between the strong absorption of red electromagnetic radiation and the strong scatter of near infrared radiation. The normalized difference vegetation index (NDVI) is one of the most often used in many applications relevant to analysis of biophysical parameters. However, conclusions about its value vary, depending on the use of specific biophysical parameters and the characteristics of the study area. For example, Chen (1996) evaluated a number of spectral indices for boreal forests and concluded that NDVI was best correlated with LAI. Gong et al. (1995) found that NDVI and LAI were positively correlated with coniferous forest. However, other studies found a weak correlation between LAI and NDVI (Nemani et al., 1993; Franklin et al., 1997; Eklundh et al., 2001). A significant statistical relationship between vegetation indices and green biomass was found (Hardisky et al., 1984), but other studies also reported little or no association between them (Anderson and Hanson, 1992; Anderson et al., 1993). Hall et al. (1995) found that NDVI was not a reliable predictor of biophysical parameters for the dominant coniferous species of the boreal forest because NDVI was linear in the sunlit canopy fraction ($R^2 = 0.96$) and the sunlit canopy fraction was not strongly correlated with biomass density. Sader et al. (1989) found that NDVI differences were not detectable for successional vegetations older than approximately 15–20 years and biomass differences in young successional tropical forests were not detectable using NDVI. The NDVI did not appear to be a good predictor of stand structure variables (height, diameter of main stem) or total biomass in uneven age and mixed broadleaf forests. Roy and Ravan (1996) discovered that the TM greenness, NDVI, and TM band 4 were related to canopy pigmentation and growth condition, and, thereby, sensi-

tive to phenological changes. NDVI and TM band 4 were not significantly correlated with biomass. However, Tucker et al. (1983) found that the integrated vegetation index could be related directly to vegetation amount (aboveground biomass) and primary productivity. It is possible to use remote-sensing canopy reflectance models for estimating foliage, woody biomass, and productive potential (Franklin and Hiernaux, 1991). Huete et al. (1997) indicated that NDVI spectrally saturated over forested areas and was sensitive to canopy background reflectance change. Boyd et al. (1996) found weak correlations between NDVI and biophysical properties in tropical forests; however, those vegetation indices derived from middle or thermal infrared wavelengths were correlated strongly with the regeneration stage of tropical forests.

McDonald et al. (1998) found that vegetation indices were significantly affected by exogenous effects, including solar zenith angle, background reflectance, stand structure, and LAI. The global environmental monitoring index (GEMI) performed best when vegetation cover was sparse, where a decrease in the value of GEMI corresponded to an increase in crown cover (McDonald et al., 1998). The perpendicular vegetation index (PVI), soil adjusted vegetation index (SAVI), transformed SAVI (TSAVI), and GEMI partially reduced background reflectance effects in the data. SAVI and TSAVI perform best when vegetation cover was dense since these indices have large dynamic ranges and small susceptibility to atmospheric perturbations (McDonald et al., 1998). Eastwood et al. (1997) found that MSAVI (modified SAVI) and GEMI were the best indices to use for salt marsh vegetation monitoring. The sensitivity of some vegetation indices to variations in canopy conditions was evaluated by Vygodskaya et al. (1989) and more than 40 indices were reviewed by Bannari et al. (1995). Treitz and Howarth (1999) summarized a variety of ratio-based indices for biophysical studies and factors affecting spectral response of forest canopies. Vegetation indices were sensitive to internal (such as canopy geometry, terrain factors, species composition) and external factors (sun elevation angle, zenith view angle, atmospheric conditions) that affected vegetation reflectance (Treitz and Howarth, 1999).

Spectral brightness showed a strong correlation with biomass values (Franklin, 1986; Roy and Ravan, 1996). The brightness and greenness from tasseled cap transform of TM image were highly sensitive to topographic variation, but they also captured much of the spectral variability associated with major changes in cover types. The wetness component from a tasseled cap transform of TM images was an important spectral variable for distinguishing among classes of closed-canopy coniferous forests (Cohen et al., 1995) and it displayed high correlation with stand attributes (Cohen and Spies, 1992). The standard deviation of tree size, mean size and density of trees in the upper canopy layers, the structural complexity index, and stand age can be most reliably estimated by analyzing satellite data (Cohen and Spies, 1992).

3. Characteristics of the study areas

Three study areas in the eastern Brazilian Amazon basin – Altamira, Bragantina, and Ponta de Pedras (hereafter, Pedras) – were selected for this research (Fig. 1). They have different soil conditions, land-use histories, landscape complexities, vegetation stand structures, and human activities, representing typical study areas in the Amazon basin (Table 1).

The Altamira study area is located along the Trans-Amazon Highway in the Brazilian state of Pará with a combination of flat and rugged terrain. The elevation ranges from 50 to 300 m. The city of Altamira and the Xingu River anchor the eastern edge of the study area. In the 1950s, an effort was made to attract colonists from northeast Brazil, who came and settled along streams as far as 20 km from the city center. With the construction of the TransAmazon Highway in the 1970s, the population and older Caboclo settlers from earlier rubber eras claimed land along the new highway and legalized their land claims (Moran, 1981). Early settlement was driven by geopolitical goals and political economic policies whose aim was to transfer production of staples like rice, corn and beans from the most southern Brazilian states to more northerly regions. The dominant native types of vegetation in this area are mature moist forest and liana forest. The main tree species are *Cecropia palmate*, *Cecropia obtuse*, *Inga alba*, and *Banara guianensis*. Most of the successional vegetations are between 8 and 17 years and the average biomass growth rate in Altamira is about 1.3 kg/m^2/year. Different stages of succes-

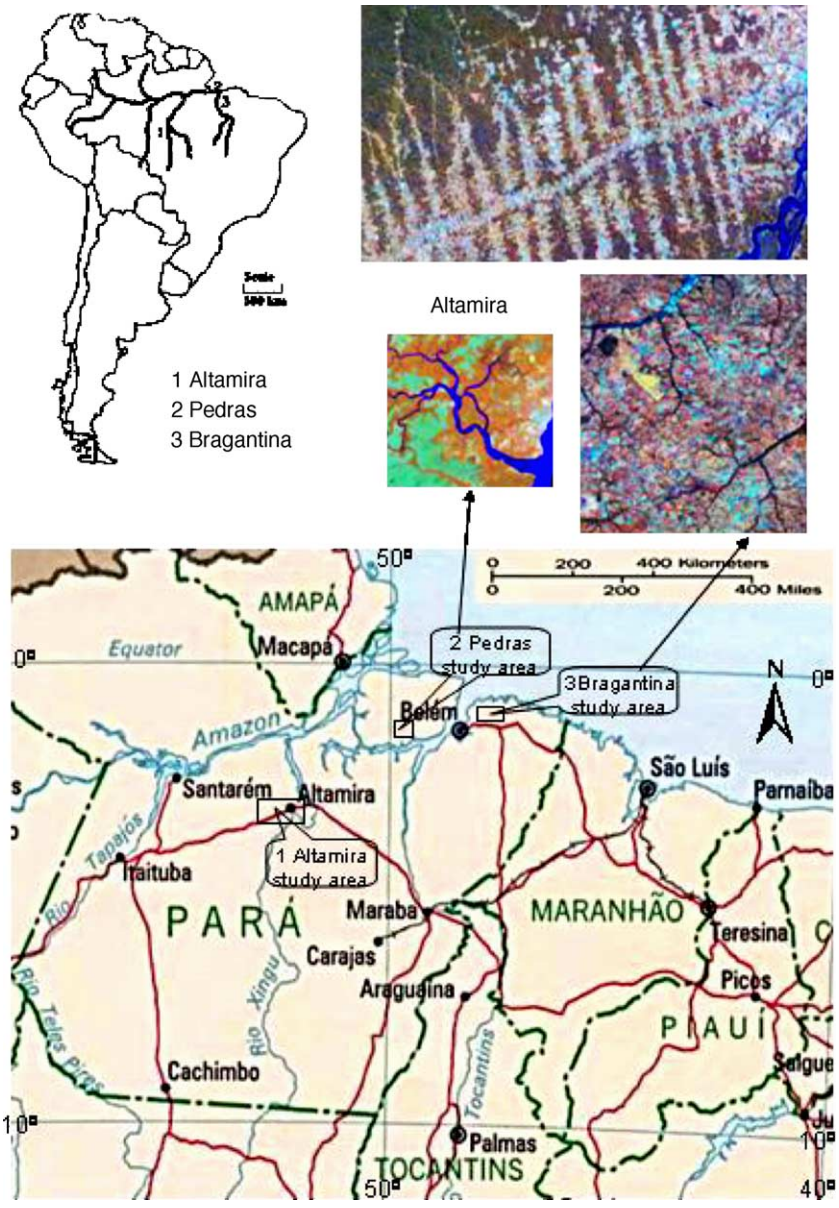

Fig. 1. Locations of three study areas and Thematic Mapper images illustrating the characteristics of the landscapes.

sional vegetations are common along the TransAmazon highway and its fish bone pattern feeder roads. Nutrient-rich alfisols, as well as nutrient-poor ultisols and oxisols are present in this study area. Annual rainfall in Altamira is approximately 2000 mm which is concentrated from late October through early June. The average annual temperature is approximately 26 °C.

The Bragantina study area is also located within the state of Pará and it has a flat topography interspersed by river channels that seasonally flood. The vegetation in this region is mostly composed of pasture and cropland, secondary growth forest, flooded forest, and a few remaining areas of dense mature forest. The main tree species are *Vismia guianensis*, *Croton matourensis*, *Maximiliana maripa*, *Guatteria peop-*

Table 1
Comparison of selected biophysical and land use characteristics in three study areas

	Altamira	Bragantina	Pedras
Soil types	Dominated by nutrient-rich alfisols. Some nutrient-poor ultisols and oxisols are also found	Mosaic of nutrient-poor soils: oxisols and ultisols	Transitional environment with upland nutrient-poor oxisols and floodplain alluvial soils
Landscape characteristics	Extensive deforestation occurred in the past 30 years. Various stages of successional vegetations are distributed along the TransAmazon highway and feeder roads	Dominated by various successional stages; some mature forests are distributed along the rivers	Dominated by dense upland forest, floodplain forest, and natural grassland
Main tree species	*C. palmate*, *C. obtuse*, *I. alba*, *B. guianensis*	*V. guianensis*, *C. matourensis*, *M. maripa*, *T. guianensis*	*C. matourensis*, *M. maripa*, *B. crispa*, *Piriquiteira*
Average vegetation age	Most successional vegetations are between 8 and 17 years	Most successional vegetations are between 10 and 25 years, with some over 40 years	Most successional vegetations less than 15 years
Vegetation stand structure	Complex	Relatively simple	Complex
Average biomass growth rate	About 1.27 kg/m^2/year for successional vegetations	About 0.59 kg/m^2/year for successional vegetations	About 0.91 kg/m^2/year for successional vegetations
Climate conditions	Rainfall: 2000 mm Rainy season: October–June Average Ann. temperature 26 °C	2200–2800 mm December–August 25–26 °C	3000 mm December–early May 27 °C
Topographic variability	Mixture of flat and rugged terrains. The elevation ranges from 50 to 300 m	Flat	Flat

pigiana, and *Tapirira guianensis*. At the beginning of twentieth century, almost one million hectares of dense tropical rain forest covered the Bragantina region; however, less than two percent of these forests remained by 1960. The dense forest that once surrounded the town of Castanhal had an average height of 23 m. Heavy occupation of this region has eliminated almost all dense forests and transformed the landscape into a mosaic comprised of a variety of succession vegetations (Tucker et al., 1998). Currently, successional vegetations, most often between 10 and 25 years, dominate the landscape. The average biomass growth rate of successional vegetations in Bragantina is 0.59 kg/m^2/year. This area is dominated by nutrient-poor soils (i.e., oxisols and ultisols). Annual rainfall ranges from 2200 to 2800 mm with a September to June concentration. The average annual temperature is 25–26 °C.

The Pedras study area is located in the estuarine region of the Amazon on Marajo Island in the municipality of Ponta de Pedras in the state of Pará. It is a topographically flat transitional region between two macro-environments with dense floodplain forests to the west and the more prominent natural savanna grasslands to the east. The vegetation has a complex structure and is rich in palms. The forest presents uniform stratification consisting of large trees with an emergent canopy reaching 35 m and a sparse herbaceous layer. Disturbed areas, whether floodplain or upland forest quickly become secondary forests with diverse stages of regrowth. Savannas mainly consist of trees 2–5 m in height that are widely spread across a mantle of grasses such as *Aristida* and *Eragrostis*. A transitional forest is located in the ecotone between forest and savanna and is characterized by lianas and palms such as *Desmoncus orthocantus* and *Mauritia martiana*. In this study area the main tree species are *C. matourensis*, *Maimiliana maripa*, *B. crispa*, and *Piriquiteira*. Most of successional vegetations are less than 15 years. The average biomass growth rate of successional vegetations in Pedras is approximately 0.91 kg/m^2/year. Floodplain alluvial soils and upland oxisols are dominant in this study area. The annual average temperature is approximately 27 °C, and rainfall is about 3000 mm per year with the wet season stretching from December to the beginning of May.

Land use varies among the three study areas, but in most cases they are variations of swidden agriculture, agroforestry, and pasture management. Altamira has experienced high rates of deforestation and succession associated with implementation of agropastural projects. The Pedras sites at Marajo Island has been historically occupied by Caboclo populations, mainly devoted to agroforestry activities in the floodplain and swidden agriculture in the uplands, although pasture and mechanized agriculture can be found in the upland oxisols. Land use in the Bragantina region has experienced several phases, and currently short-fallow swidden cultivation and pasture development dominate. Cultivation of secondary growth areas has been common for decades, and islands of mature forest are rare (Moran et al., 2002). The long settlement history, high human population density, and repeated land clearing (including burning), over the past century in Bragantina has degraded the landscape, leading to slower vegetation regrowth rate.

4. Methods

4.1. Field data collection and analysis

A nested sampling strategy, organized by region, site, plot, and subplot, was employed to inventory vegetation data (Fig. 2). The region represents the study area that included all sample sites. The site in this region was selected for plot sampling. Sites were selected to represent a particular age class and land use history. The first step for sampling was to visit the study area to assess its level of homogeneity. The size of sites varied according to the land use activity previously in place, ranging from a minimum of two hectares (e.g., swidden agriculture area) to several hundred hectares (mature forest). The field survey sites were determined based on a stratified random strategy using TM classification images. Once a site was selected and demarcated for sampling, plots were randomly located along one or more transects and

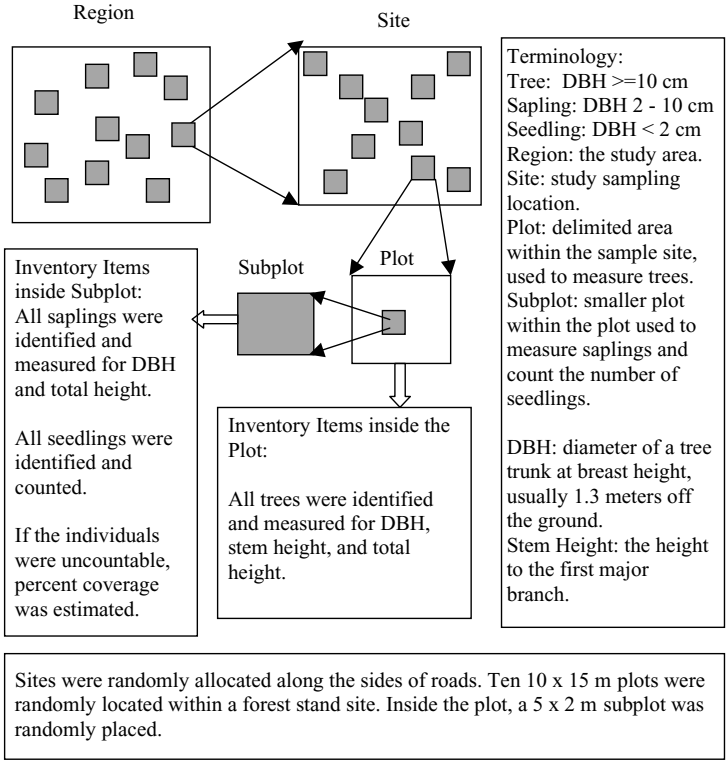

Fig. 2. Design of field data collection.

subplots were located randomly inside the plots. The distance between plots varied, depending on the size, shape, and location of the site (e.g., previous land use activities and presence of micro-topographic environments). In general, 10 plots (10 m × 15 m for each plot) in each site were allocated and one randomly selected subplot (5 m × 2 m for each subplot) was nested within each plot. Plots were designed to inventory trees, and subplots were used to inventory saplings, seedlings, and herbaceous species. In each plot, all individual trees with a diameter at breast height greater than 10 cm were identified and measured for DBH, stem height (the height of the first major branch), and total height. In the subplot, all saplings (DBH between 2 and 10 cm), seedlings (DBH less than 2 cm), and herbaceous vegetation (percent of ground cover) were identified and counted. The diameter and total height were recorded for all individuals with DBH between 2 and 10 cm.

Fieldwork was conducted during the dry season in 1992 and 1993 in Altamira and Pedras, and in 1994 and 1995 in Bragantina. During the fieldwork, Landsat TM color composites were used to allocate the samples sites and GPS devices were used to identify the coordinates of each site. Table 2 provides a summary of collected data in these three study areas and Table 3 provides statistics of the selected forest stand parameters (average stand diameter and height, basal area, and aboveground biomass) based on the site level.

An Oracle database was developed to store and manage the vegetation inventory data. The Amazon-database-information system software was developed using visual basic language to analyze the vegetation stand parameters. In this research, Eq. (1) (Nelson et al., 1999) was used to calculate biomass for those trees and saplings with DBHs of less than 25 cm, and Eq. (2) (Overman et al., 1994) was used to calculate biomass for those trees with DBHs greater than or equal to 25 cm. Four forest stand parameters were calculated using Eqs. (3)–(6) at the site level:

$$\ln(\mathrm{DW1}) = -2.5202 + 2.1400\ln(D) + 0.4644\ln(H) \quad (1)$$

Table 2
Summary of data collected from three study areas

	Altamira	Bragantina	Pedras
Quantity of			
Sites	20[a]	18	14
Plots[b]	131	126	81
Subplots	239	215	187
Trees	1572	989	1527
Saplings	744	1085	1060
Seedlings	9593	13461	7129
Field data collection date	1992, 1993	1994, 1995	1992, 1993
Acquisition date of TM images	20 July 1991	21 June 1994	22 July 1991

[a] Four sites had coordinate errors. Only 16 sites were used in this research.
[b] Some sites of young successional vegetation do not have plots because of no trees with DBH greater than 10 cm.

Table 3
Summary statistics for field sample data in the three study areas

Study area	Variables	Sites	Minimum	Maximum	Mean	S.D.
Altamira	AGB	20	0.828	51.675	13.636	12.783
	BA	20	1.285	80.406	23.568	19.378
	ASD	20	2.298	29.990	14.800	9.559
	ASH	20	2.458	20.265	10.164	5.504
Bragantina	AGB	18	1.697	30.825	9.503	8.598
	BA	18	0.261	51.061	18.143	13.922
	ASD	18	2.039	25.474	13.647	7.791
	ASH	18	2.400	18.936	9.916	4.776
Pedras	AGB	14	2.408	39.467	12.048	10.548
	BA	14	5.247	49.525	21.794	12.224
	ASD	14	2.634	39.266	16.749	11.474
	ASH	14	2.470	20.089	10.320	6.477

AGB, aboveground biomass; BA, basal area; ASD, average stand diameter; ASH, average stand height.

$$\ln(\mathrm{DW2}) = -3.843 + 1.035\ln(D^2H) \quad (2)$$

Average stand diameter (ASD, cm):

$$\mathrm{ASD} = \sqrt{\frac{\left[\left(\sum_{i=1}^{s}\mathrm{DS}^2\right)\mathrm{PA}/\mathrm{SPA} + \sum_{j=1}^{m+n}\mathrm{DT}^2\right]}{s+m+n}} \quad (3)$$

Average stand height (ASH, m):

$$\mathrm{ASH} = \frac{\left[\left(\sum_{i=1}^{s}\mathrm{HS}\right)\mathrm{PA}/\mathrm{SPA} + \sum_{j=1}^{m+n}\mathrm{HT}\right]}{s+m+n} \quad (4)$$

Basal area (BA, m^2/ha):

$$\mathrm{BA} = \frac{\sum_{i=1}^{s}\mathrm{BAS}}{\mathrm{SPA}} + \frac{\sum_{j=1}^{m+n}\mathrm{BAT}}{\mathrm{PA}} \quad (5)$$

Aboveground biomass (AGB, kg/m^2):

$$\mathrm{AGB} = \frac{\sum_{i=1}^{m}\mathrm{DW1}_i + \sum_{j=1}^{n}\mathrm{DW2}_j}{\mathrm{PA}} + \frac{\sum_{k=1}^{s}\mathrm{DW1}_k}{\mathrm{SPA}} \quad (6)$$

In these equations, ln is the natural logarithm, D the diameter at breast height (cm), and H the total tree height (m). DS, HS, and BAS are sapling DBH, height, and basal area, respectively. DT, HT, and BAT are tree DBH, height, and basal area, respectively. DW1 is individual tree or sapling biomass (kg) when DBH is less than 25 cm, DW2 is the individual tree biomass when DBH is greater than or equal to 25 cm, m the total tree number in a plot when DBH is between 10 and 25 cm, n the total tree number in a plot when DBH is greater than or equal to 25 cm, and s the total sapling number in a subplot area when DBH is between 2 and 10 cm. PA and SPA are the total plot area and subplot area (m^2) within the selected site, respectively.

4.2. Image preprocessing and development of vegetation indices

Geometrical rectification and radiometric and atmospheric correction of remotely sensed data are often required for many applications (Lu et al., 2002b). The importance of accurate geometric rectification is obvious because the image data are often related to ground truth data or used for further analysis through combination of different sources of data. In this research, TM images were acquired in July 1991 for Altamira and Pedras and June 1994 for Bragantina. These images were geometrically rectified into UTM projection using control points taken from topographic maps at 1:100,000 scale. A nearest-neighbor resampling technique was used and a root mean square error of less than 0.5 pixel was obtained for each TM image.

A variety of methods have been used for atmospheric normalization or correction (Markham and Barker, 1987; Gilabert et al., 1994; Chavez, 1996; Stefan and Itten, 1997; Vermote et al., 1997; Song et al., 2001). Different models have their own characteristics and requirements for the input parameters. Which method is suitable for a specific project depends on the objective of the study and atmospheric data available. For many historical remote-sensing data, atmospheric data at the time of image acquisition are not available. In this situation, advanced calibration methods such as 6S are difficult to use for atmospheric correction. However, image-based calibration methods, such as an improved image-based dark object subtraction (DOS) model, are very suitable to use for atmospheric correction of historical image data (Lu et al., 2002b). In this research, all TM images collected have very good quality and are devoid of clouds over the study areas. The terrains in these study areas are predominantly flat, hence, atmospheric effects can be regarded as uniform. An improved image-based DOS model was used in this study. The gain and offset, and sun elevation angle were obtained from the TM image header file. The path radiance was identified based on clear water as the standard for each band. The atmospheric transmittance values for visible and near infrared bands were derived from Chavez (1996), which were an average for each spectral band derived from the radiative transfer code. For middle infrared bands, the atmospheric transmittance was set to one. Surface reflectance values after calibration fall within the range between 0 and 1, but for convenience of data analysis, these values were rescaled to a range between 0 and 100 by multiplying each pixel by 100.

After geometric rectification and atmospheric calibration, a variety of vegetation indices were calculated separately for each study area. These vegetation indices, grouped into four categories for a convenience of analysis, are summarized in Table 4. These included

Table 4
Image variables used in research

Vegetation indices	Formula
Simple ratio	
TM4/3	TM4/TM3
TM5/3	TM5/TM3
TM5/4	TM5/TM4
TM5/7	TM5/TM7
Normalized vegetation indices	
NDVI	(TM4 − TM3)/(TM4 + TM3)
ND53	(TM5 − TM3)/(TM5 + TM3)
ND54	(TM5 − TM4)/(TM5 + TM4)
ND57	(TM5 − TM7)/(TM5 + TM7)
ND32	(TM3 − TM2)/(TM3 + TM2)
Complex vegetation indices	
ARVI	(NIR − 2 RED + BLUE)/(NIR + 2 RED − BLUE)
ASVI	$((2\,\mathrm{NIR}+1)-\sqrt{(2\mathrm{NIR}+1)^2-8(\mathrm{NIR}-2\,\mathrm{RED}+\mathrm{BLUE})})/2$
SAVI	$((\mathrm{NIR}-\mathrm{RED})/(\mathrm{NIR}+\mathrm{RED}+\mathrm{L}))(1+\mathrm{L})$
MSAVI	$((2\,\mathrm{NIR}+1)-\sqrt{(2\,\mathrm{NIR}+1)^2-8(\mathrm{NIR}-2\,\mathrm{RED})})/2$
GEMI	$\xi(1-0.25\xi)-((\mathrm{RED}-0.125)/(1-\mathrm{RED}))$, where $\xi=(2(\mathrm{NIR}^2-\mathrm{RED}^2)+1.5\,\mathrm{NIR}+0.5\,\mathrm{RED})/(\mathrm{NIR}+\mathrm{RED}+0.5))$
Image transform	
VIS123	TM1 + TM2 + TM3
MID57	TM5 + TM7
Albedo	TM1 + TM2 + TM3 + TM4 + TM5 + TM7
KT1	0.304TM1 + 0.279TM2 + 0.474TM3 + 0.559TM4 + 0.508TM5 + 0.186TM7
KT2	−0.285TM1 − 0.244TM2 − 0.544TM3 + 0.704TM4 + 0.084TM5 − 0.180TM7
KT3	0.151TM1 + 0.197TM2 + 0.328TM3 + 0.341TM4 − 0.711TM5 − 0.457TM7
PC1-A	0.054TM1 + 0.130TM2 + 0.143TM3 + 0.595TM4 + 0.709TM5 + 0.321TM7
PC2-A	−0.079TM1 − 0.121TM2 − 0.212TM3 + 0.787TM4 − 0.421TM5 − 0.372TM7
PC3-A	0.230TM1 + 0.504TM2 + 0.616TM3 + 0.140TM4 − 0.472TM5 + 0.266TM7
PC1-P	0.056TM1 + 0.079TM2 + 0.127TM3 − 0.845TM4 − 0.490TM5 − 0.143TM7
PC2-P	−0.052TM1 − 0.060TM2 − 0.162TM3 + 0.472TM4 − 0.745TM5 − 0.436TM7
PC3-P	0.327TM1 + 0.617TM2 + 0.663TM3 + 0.233TM4 − 0.116TM5 − 0.079TM7
PC1-B	0.140TM1 + 0.242TM2 + 0.313TM3 + 0.262TM4 + 0.739TM5 + 0.457TM7
PC2-B	−0.062TM1 − 0.026TM2 − 0.170TM3 + 0.952TM4 − 0.108TM5 − 0.222TM7
PC3-B	0.276TM1 + 0.502TM2 + 0.674TM3 + 0.069TM4 − 0.439TM5 − 0.140TM7

ND, normalized difference; ARVI, atmospherically resistant vegetation index; ASVI, atmospheric and soil vegetation index; SAVI, soil adjusted vegetation index; MSAVI, modified SAVI; GEMI, global environmental monitoring index; VIS, visible wavelengths (TM1, TM2, TM3), MID, middle infrared wavelengths (TM5, TM7); PC, principle component analysis; KT, tasseled cap transform.

(1) simple ratios: TM4/3, TM5/3, TM5/4, and TM5/7; (2) normalized ratios: NDVI, ND54, ND53, ND57, and ND32; (3) complex vegetation indices: atmospherically resistant vegetation index (ARVI), atmospheric and soil vegetation index (ASVI), SAVI, MSAVI, and GEMI; and (4) linear transform of multiple bands: VIS123, MID57, albedo, tasseled cap (KT) transform, and unstandardized principal component analysis (PCA).

4.3. Integration of field data and TM spectral responses

All the sample data have accurate coordinates derived from GPS devices and were located on geometrically rectified TM color composites during the fieldwork. These sample data can be linked to TM individual bands or the vegetation indices derived from TM image to extract the spectral responses for

each sample site. The selected forest stand parameters were aggregated from 10 plots and 10 subplots to represent forest stand features within each site. A window size of 3 by 3 was used to extract the mean value of spectral responses for each site. Stand parameters, such as ASD, ASH, and AGB, from each site were associated with spectral responses using a Pearson's correlation coefficient analysis to explore the forest stand parameter and TM spectral response relationships. The coefficient measures the strength of linear relationships between two variables. One variable is a forest stand parameter, such as ASD, ASH, or AGB; and another variable is the spectral response from a single TM band or a vegetation index.

4.4. Impacts of forest stand structures on relationships between forest stand parameters and spectral responses

Tree species composition, forest stand structures and associated canopy shadows, and vegetation vigor, are regarded as important factors affecting vegetation reflectance (Lu, 2001). Reflectance among the sites with similar biomass amounts often varies and comparison of different stand structures may be an effective way to explore how the different forest stand characteristics affect vegetation reflectance. Graphs illustrating the reflectance change with wavelengths were used to analyze biomass growth impacts on vegetation reflectance. The tree height distributions were compared for those sites with similar biomass amounts in the three study areas. Because Altamira and Bragantina represent two extremes in forest stand structures, the analysis in this paper is mainly focused on these two study areas.

5. Results and discussion

5.1. Relationships between forest stand parameters and TM reflectance

Selected forest stand parameters have negative correlations with TM reflectance and such relationships vary depending on the characteristics of the study areas. Table 5 summarizes the correlation coefficients between the selected forest stand parameters and TM spectral signatures in the three study areas.

In Altamira, middle infrared wavelengths were the bands most significantly (negatively) correlated with

Table 5
Correlation coefficients between selected forest stand parameters and TM bands

Regions	Band	AGB	BA	ASD	ASH
Altamira (16 sites)	TM1	−0.524[a]	−0.352	−0.577[a]	−0.736[b]
	TM2	−0.509	−0.432	−0.670[b]	−0.828[b]
	TM3	−0.501	−0.415	−0.683[b]	−0.813[b]
	TM4	−0.538[a]	−0.509	−0.618[a]	−0.655[a]
	TM5	−0.627[a]	−0.576[a]	−0.794[b]	−0.851[b]
	TM7	−0.606[a]	−0.595[a]	−0.806[b]	−0.839[b]
Bragantina (18 sites)	TM1	−0.597[a]	−0.637[b]	−0.698[b]	−0.708[b]
	TM2	−0.741[b]	−0.781[b]	−0.861[b]	−0.876[b]
	TM3	−0.618[b]	−0.662[b]	−0.757[b]	−0.758[b]
	TM4	−0.837[b]	−0.794[b]	−0.814[b]	−0.833[b]
	TM5	−0.810[b]	−0.802[b]	−0.832[b]	−0.861[b]
	TM7	−0.668[b]	−0.685[b]	−0.745[b]	−0.771[b]
Pedras (14 sites)	TM1	−0.629[a]	−0.598[a]	−0.635[a]	−0.714[b]
	TM2	−0.685[b]	−0.658[a]	−0.675[a]	−0.766[b]
	TM3	−0.625[a]	−0.598[a]	−0.628[a]	−0.709[b]
	TM4	−0.756[b]	−0.762[b]	−0.750[b]	−0.786[b]
	TM5	−0.826[b]	−0.781[b]	−0.832[b]	−0.922[b]
	TM7	−0.786[b]	−0.789[b]	−0.801[b]	−0.879[b]

[a] Correlation is significant at the 0.05 level.
[b] Correlation is significant at the 0.01 level.

AGB and BA and they also had strong negative correlations with ASD and ASH. The visible wavelengths were not significantly correlated with AGB and BA; however, they are strongly correlated with ASD and ASH. The near infrared wavelength appeared to have a relatively weak correlation with selected stand parameters compared with middle infrared wavelengths. In Bragantina, TM4, TM5, and TM2 were the best bands that most strongly correlated with all selected forest stand parameters. TM1, TM3, and TM7 exhibited statistical significance, but had relatively weak, correlations with forest stand parameters compared with TM4, TM5, and TM2 correlations. In Pedras, all selected forest stand parameters were significantly correlated with TM bands. Middle infrared and near infrared wavelengths were the best image bands most strongly (negatively) correlated with AGB, BA, ASD, and ASH. The visible bands were also significantly correlated, but they had relatively weak relationships to the stand parameters compared with near and middle infrared bands.

In all three study areas, ASD and ASH had higher correlations with TM bands than did AGB and BA, implying that there is a different capability of TM spectral signatures for forest stand parameter estimation. Considering all non-thermal TM bands, TM5 and TM7 are the most strongly correlated with ASD and ASH, somewhat independent of the characteristics of the study areas. In particular, bands TM5 and TM7 are the best bands to use in Altamira and Pedras with their more complex forest stand structures. In Bragantina, with a relatively simple stand structure, bands TM2 and TM4 were also strongly correlated with ASD and ASH, implying that TM2 and TM4 may be more sensitive to the forest stand structures. Band TM5 in Pedras or TM4 in Bragantina is suitable for AGB or BA estimation, but TM spectral signatures may be not suitable for AGB and BA estimation in Altamira.

The forest stand parameters have higher correlations with TM bands in Bragantina and Pedras than in Altamira, indicating the impacts of different characteristics of the study areas on the forest stand parameter and TM reflectance relationships. The complex stand structure in Altamira may be an important factor reducing relationships between TM spectral signatures and AGB and BA because AGB and BA are comprehensive parameters that are related to forest stand density, vegetation age, and species composition, in addition to the DBH and height. The optical sensors mainly capture canopy information and the ASD and ASH are more strongly correlated with the canopy. This results in better relationships of TM spectral signatures with ASD and ASH than with AGB and BA in different study areas.

5.2. Relationships between forest stand parameters and vegetation indices

Not all vegetation indices are significantly related to forest stand parameters. Also vegetation indices are not definitely better related to forest stand parameters than TM spectral signatures. Table 6 summarizes the correlation coefficients between forest stand parameters and vegetation indices in the three study areas.

The simple ratio image, TM5/4, was significantly correlated with AGB and BA and strongly correlated with ASD and ASH in Altamira. In Bragantina all the selected simple ratio-based indices, except TM5/4, were significantly correlated with selected forest stand parameters, but in Pedras, only TM5/7 was significant. The normalized vegetation index, ND54, was significantly correlated with AGB and BA and strongly correlated with ASD and ASH in Altamira. In Bragantina ND32 is significantly correlated with AGB and BA and all vegetation indices used in this study are significantly correlated with ASD and ASH. In Pedras, only ND57 is significantly correlated with selected stand parameters. In the category of complex vegetation indices, no vegetation indices, except GEMI, are strongly correlated with stand parameters used in this study. However, in Bragantina, these vegetation indices are significantly correlated with ASD and ASH. In contrast to simple ratios, normalized or complex vegetation indices, the linearly transformed images, i.e., MID57, albedo, KT1, KT3, and PC1, are significantly correlated with AGB and BA and strongly correlated with ASD and ASH in Altamira. In Pedras and Bragantina, MID57, albedo, KT1, and PC1 are strongly correlated with the forest stand parameters selected. PC3 in Pedras and PC2 in Bragantina are also strongly correlated with the stand parameters selected. Overall, the vegetation indices from linearly transformed images provided higher correlation coefficients than other categories of vegetation indices (simple ratios, normalized indices, and complex indices) in the three study areas. In Altamira

Table 6
Correlation coefficients between vegetation indices and selected forest stand parameters in the study areas

VI	Altamira				Bragantina				Pedras			
	AGB	BA	ASD	ASH	AGB	BA	ASD	ASH	AGB	BA	ASD	ASH
TM4/3	0.124	0.008	0.260	0.411	0.505[a]	0.530[a]	0.607[a]	0.661[a]	0.243	0.199	0.276	0.354
TM5/3	−0.474	−0.487	−0.519[a]	−0.441	0.511[a]	0.528[a]	0.628[a]	0.677[a]	−0.060	−0.053	−0.048	−0.028
TM5/4	−0.624[a]	−0.526[a]	−0.817[b]	−0.881[b]	−0.404	−0.464	−0.499	−0.526[a]	−0.445	−0.364	−0.456	−0.554[a]
TM5/7	0.466	0.524[a]	0.660[a]	0.625[a]	0.476	0.518[a]	0.586[a]	0.620[a]	0.591[a]	0.675[a]	0.638[a]	0.686[a]
NDVI	0.157	0.035	0.308	0.458	0.459	0.521[a]	0.625[a]	0.633[a]	0.247	0.205	0.259	0.337
ND53	−0.485	−0.499	−0.534[a]	−0.470	0.447	0.500	0.627[a]	0.632[a]	−0.033	−0.018	−0.018	0.001
ND54	−0.635[a]	−0.540[a]	−0.833[b]	−0.908[b]	−0.420	−0.470	−0.488	−0.519[a]	−0.436	−0.354	−0.450	−0.550[a]
ND57	0.486	0.545[a]	0.687[a]	0.652[a]	0.459	0.497	0.572[a]	0.601[a]	0.589[a]	0.675[a]	0.625[a]	0.671[a]
ND32	0.200	0.110	0.321	0.284	−0.628[a]	−0.615[a]	−0.561[a]	−0.612[a]	−0.002	−0.003	0.081	0.060
ARVI	0.194	0.113	0.394	0.523[a]	0.530[a]	0.578[a]	0.686[a]	0.699[a]	0.166	0.127	0.177	0.246
ASVI	0.192	0.119	0.401	0.529[a]	0.493	0.553[a]	0.662[a]	0.669[a]	0.156	0.121	0.166	0.234
SAVI	0.123	0.008	0.271	0.420	0.434	0.500	0.605[a]	0.611[a]	0.224	0.181	0.235	0.311
MSAVI	0.157	0.037	0.307	0.456	0.435	0.503	0.608[a]	0.613[a]	0.239	0.195	0.245	0.321
GEMI	0.482	0.464	0.535[a]	0.553[a]	0.787[b]	0.740[b]	0.747[b]	0.767[b]	0.666[a]	0.684[a]	0.662[a]	0.676[a]
VIS123	−0.529[a]	−0.427	−0.684[a]	−0.837[b]	−0.681[a]	−0.723[b]	−0.807[b]	−0.816[b]	−0.657[a]	−0.628[a]	−0.655[a]	−0.740[b]
MID57	−0.624[a]	−0.583[a]	−0.801[b]	−0.851[b]	−0.773[b]	−0.773[b]	−0.813[b]	−0.841[b]	−0.822[b]	−0.790[b]	−0.830[b]	−0.918[b]
Albedo	−0.609[a]	−0.560[a]	−0.755[b]	−0.819[b]	−0.818[b]	−0.813[b]	−0.859[b]	−0.881[b]	−0.816[b]	−0.798[b]	−0.816[b]	−0.890[b]
KT1	−0.600[a]	−0.553[a]	−0.734[b]	−0.795[b]	−0.835[b]	−0.821[b]	−0.862[b]	−0.883[b]	−0.819[b]	−0.803[b]	−0.818[b]	−0.886[b]
KT2	−0.488	−0.475	−0.538[a]	−0.547[a]	−0.762[b]	−0.688[a]	−0.672[a]	−0.693[a]	−0.644[a]	−0.661[a]	−0.635[a]	−0.644[a]
KT3	0.619[a]	0.584[a]	0.849[b]	0.880[b]	0.333	0.361	0.368	0.407	0.218	0.159	0.242	0.314
PC1	−0.603[a]	−0.562[a]	−0.741[b]	−0.790[b]	−0.815[b]	−0.809[b]	−0.851[b]	−0.876[b]	0.815[b]	0.811[b]	0.816[b]	0.867[b]
PC2	−0.126	−0.132	−0.001	0.024	−0.797[b]	−0.741[b]	−0.751[b]	−0.766[b]	0.438	0.369	0.459	0.558[a]
PC3	0.300	0.311	0.355	0.246	−0.058	−0.177	−0.335	−0.276	−0.742[b]	−0.729[b]	−0.735[b]	−0.806[b]

[a] Correlation is significant at the 0.05 level.
[b] Correlation is significant at the 0.01 level.

and Pedras, the vegetation indices that included TM4 and TM3 in their formulas, such as ARVI, ASVI, MSAVI, SAVI, NDVI, and TM4/3, have weak statistical relationships with forest stand parameters, especially AGB and BA. However, vegetation indices including TM5, such as ND54, ND53, ND57, TM5/3, TM5/4, and TM5/7, have better correlations with forest stand parameters. In contrast, this conclusion is not true in Bragantina.

The ASD and ASH had higher correlations with vegetation indices than AGB and BA in all three study areas, suggesting that different vegetation indices have different potentials for estimation of relevant forest stand parameters. In general, the correlation coefficients in Bragantina and Pedras are higher than in Altamira. This implies that different biophysical environments influence relationships between vegetation indices and selected stand parameters. Three categories of vegetation indices can be roughly grouped according to statistical relationships between vegetation indices and forest stand parameters in these three study areas: (1) vegetation indices that have stable and strong correlations with forest stand parameters with some independence of biophysical environments; such vegetation indices include KT1, PC1, MID57, and albedo; (2) vegetation indices that have strong correlations with forest stand parameters in a study area like Altamira that have complex stand structures (e.g. ND54, TM5/4, and KT3); and (3) vegetation indices that have weak statistical relationships with forest stand parameters and are not appropriate for research involving these parameters (such vegetation indices include most complex vegetation indices (e.g., ASVI, ARVI), NDVI, and the simple ratios that include TM3 band (e.g., TM5/3, TM4/3)).

A combinative analysis of the loadings from PCA or Tasseled cap transforms and the correlation between TM spectral signatures and forest stand parameters

can explain why the vegetation indices using linear transform have better correlations than other ratio-based vegetation indices. For example, bands TM5 and TM4 have larger loadings in KT1 and PC1 components and higher vegetation reflectance. This means that KT1 and PC1 components receive more information from TM4 and TM5, indicating that those vegetation indices derived more information from near and middle infrared wavelengths, which have higher correlations with forest stand parameters. The KT2 and PC2 components have higher loadings of TM4, indicating that more information is derived from the TM4 band, and strong correlations with forest stand parameters in Bragantina exist because relatively simple stand structures lead to TM4 having the best relationships with these parameters. However, KT2 and PC2 components have weak correlations in Altamira and Pedras because of their complex stand structures. The KT3 band receives more information from middle infrared wavelengths, which encourages good correlations with forest stand parameters in Altamira but weak correlations in Pedras and Bragantina. The PC3 band derives more information from visible bands (TM2 and TM3), thus PC3 has weak correlations with forest stand parameters in Altamira. However, Pedras and Bragantina have strong PC3 correlations with forest parameters due to different vegetation structures, land-use histories, and canopy homogeneities.

5.3. Impacts of forest stand structures on vegetation reflectance

Table 7 compares tree height distribution among those successional vegetation sites with middle-level biomass amounts in the two study areas. Forest sites with similar biomass amounts can have different tree height distribution, for instance, between Altamira sites A006 and A011 (about 13 kg/m^2) and A014 and A007 (about 10 kg/m^2). Forest sites with different biomass amounts can have similar tree height distribution, such as between A006 and A007 in Altamira. The complex tree height distribution strongly contributes to poor correlations between AGB or BA and spectral responses in Altamira. In contrast, Bragantina has a consistent trend that tree height distribution

Table 7
Comparison of tree height distribution among Altamira (A) and Brangantina (B) sites

	Site									
	A006	A011	A014	A007	A013	B001	B006	B002	B020	B024
Biom.	13.6	13.1	10.3	10.0	8.3	7.1	8.9	10.4	10.4	13.3
Age	8	10	7	8	10	14	19	20	35	25
$H < 5$	3	2	4	1	2	2	2	4		
6	2	9	7	8	2	3	1			
7	3	11	10	3	7	4	3		2	
8	3	12	14	8	8	22	1	5		1
9	13	21	13	6	25	23	4	14	4	1
10	6	22	12	6	11	10	12	16	13	6
11	5	23	16	5	12	8	12	22	5	3
12	11	13	13		9	5	12	17	12	12
13	13	6	10	8	8	1	10	3	16	6
14	16	4	8	8	4		2	4	14	7
15	15	6	3	13	5		3	8	14	9
16	9	2	2	7	4			2	17	17
17	3		1	1	1				3	6
18	4			5	2			1	1	7
19	1			2	2					4
20	4				2					
21	1				2					
22	1			1						
23		1								

Biom., aboveground biomass (kg/m^2); age, years; H, tree height (m).

becomes more complex as biomass increases. Hence, the TM spectral signatures can effectively show forest stand structure difference, leading to a high correlation with biomass. Comparison of the sites between Altamira and Bragantina indicates that the ranges of tree height distribution in Altamira are often larger than in Bragantina. In particular, some emergents with large tree DBH and tall tree height have very serious impacts on the reflectance because of their canopy shadows. This problem is more serious in Altamira than in Bragantina, as indicated in Table 7. This implies that the forest stand structure in Altamira is more complex than in Bragnatina which is the main reason why relationships between AGB or BA and TM spectral responses are much weaker in Altamira than in Bragantina. The impacts of forest stand structure can be explained more clearly using graphs of vegetation reflectance.

Figs. 3 and 4 illustrate the reflectance change due to different forest stand structures and vegetation growth. In Altamira, the trend that reflectance decreases as vegetation biomass increases is not obvious (Fig. 3), but in Bragantina this trend is very consistent (Fig. 4). Combinative analysis of Fig. 3 and Table 7 indicated that reflectance is closely related to tree height distribution, i.e., it is complex forest stand structures, rather than biomass differences, that decreased reflectance in Altamira. For example, sites A006 and A011 have similar biomass amount (13.6 versus 13.1 kg/m^2), but the stand structure in A006 is more complex than in A011. Thus, the vegetation reflectance in A006 is lower than in A011. This is especially obvious in the near infrared wavelength (TM4). A similar situation occurs between sites A014 and A007 (10.3 versus 10.0 kg/m^2). The stand structure in A007 is much more complex than in A014. Thus, the reflectance

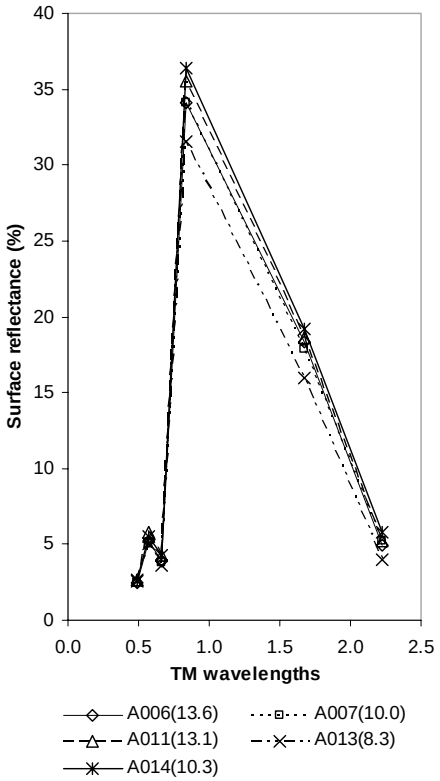

Fig. 3. Reflectance curves among different sites in Altamira illustrating impacts of forest stand structures. Note: site no. (biomass, kg/m^2).

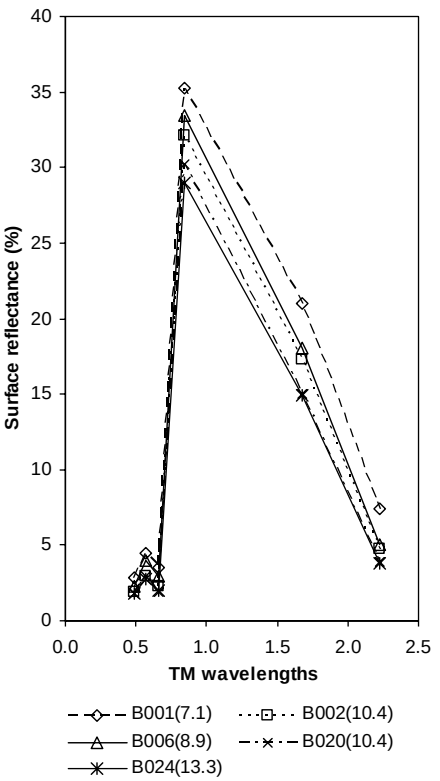

Fig. 4. Reflectance curves among different sites in Bragantina illustrating impacts of forest stand structures. Note: site no. (biomass, kg/m^2).

of A007 is much lower than A014. In contrast, A006 and A007 have different biomass amounts (13.6 versus 10.0 kg/m^2), but have similar stand structure (both have emergents), hence, their reflectance values are very similar. In Bragantina, forest stand structure become more complex as biomass increases (Table 7), thus the reflectance decreases (Fig. 4). Analysis of Figs. 3 and 4 and Table 7 indicates that the change of vegetation reflectance is directly related to forest stand structure, instead of biomass. When biomass growth has a consistent trend with stand structure change, as illustrated by Bragantina, the correlation between biomass and TM spectral responses is high. In contrast, when biomass increase is inconsistent with forest stand structure change, as in Altamira, the correlation between AGB and TM responses is poor. However, average stand height or DBH is directly related to the forest stand structure, thus TM spectral signatures have good correlations with these parameters in different study areas. This suggests that TM spectral responses are more suitable for ASD or ASH than for AGB or BA research, particularly in those study areas with complex stand structures like those found in Altamira.

Landsat TM data primarily captures canopy information instead of individual tree information due to its limited spatial resolution. The complex stand structure can also result in TM reflectance saturation because of the relatively low radiometric resolution (8 bit in TM data). This situation is especially obvious in Altamira between advanced successional and mature forests because they have similar stand structures even if their biomass amounts vary significantly. A similar conclusion was made by Steininger (2000) who found that the canopy reflectance saturated when biomass reached about 15 kg/m^2 or forest succession vegetation ages exceeded 15 years. This problem makes biomass estimation difficult for the advanced successional and mature forests in those sites with complex stand structures.

6. Conclusion

Bands TM5, PC1, KT1, albedo, and MID57 are the best spectral data forms that are strongly correlated with forest stand parameters, which are somewhat independent of different biophysical environments. These data forms are appropriate to use for research involving forest stand parameters in different study areas. The complex forest stand structures and associated canopy shadows weakened relationships between TM spectral responses and forest stand parameters. Different stand structures affect the conclusions about the relationships between TM spectral responses and biophysical parameters. These results can be used to guide the selection of suitable TM band(s) and vegetation indexes for estimating relevant biophysical parameters in moist tropical forest regions. In addition, the relationships identified provide insights into developing new complex data transformation equations that have a potential to enhance accurate classification of forest parameters. Newly derived equations will likely be valuable in implementing selected research at regional or global scales using TM or moderate resolution imaging spectroradiometer (MODIS) data.

Acknowledgements

The authors wish to acknowledge the support of the National Science Foundation (95-21918 and 93-10049), the National Institutes of Health's NICHD (9710386A), and support from NASA's LBA program through grant N005-334 that made data collection and analysis for this paper possible.

References

Ahern, F.J., Erdle, T., Maclean, D.A., Kerppeck, I.D., 1991. A quantitative relationship between forest growth rates and Thematic Mapper reflectance measurements. Int. J. Rem. Sens. 12, 387–400.

Anderson, G.L., Hanson, J.D., 1992. Evaluating handheld radiometer derived vegetation indices for estimating above ground biomass. Geocarto Int. 7, 71–78.

Anderson, G.L., Hanson, J.D., Haas, R.H., 1993. Evaluating Landsat Thematic Mapper derived vegetation indices for estimating above-ground biomass on semiarid rangelands. Rem. Sens. Environ. 45, 165–175.

Ardo, J., 1992. Volume quantification of coniferous forest compartments using spectral radiance record by Landsat Thematic Mapper. Int. J. Rem. Sens. 13, 1779–1786.

Bannari, A., Morin, D., Bonn, F., Huete, A.R., 1995. A review of vegetation indices. Rem. Sens. Rev. 13, 95–120.

Boyd, D.S., Foody, G.M., Curran, P.J., Lucas, R.M., Honzák, M., 1996. An assessment of radiance in Landsat TM middle and

thermal infrared wavebands for the detection of tropical forest regeneration. Int. J. Rem. Sens. 17, 249–261.

Butera, M.K., 1986. A correlation and regression analysis of percent canopy closure versus TMS spectral response for selected forest sites in the San Juan National Forest, Colorado. IEEE Trans. Geosci. Rem. Sens. 24, 122–129.

Castel, T., Guerra, F., Caraglio, Y., Houllier, F., 2002. Retrieval biomass of a large Venezuelan pine plantation using JERS-1 SAR data, analysis of forest structure impact on radar signature. Rem. Sens. Environ. 79, 30–41.

Chavez Jr., P.S., 1996. Image-based atmospheric corrections – revisited and improved. Photogram. Eng. Rem. Sens. 62, 1025–1036.

Chen, J.M., 1996. Evaluation of vegetation indices and a modified simple ratio for boreal applications. Can. J. Rem. Sens. 22, 229–242.

Cohen, W.B., Spies, T.A., 1992. Estimating structural attributes of Douglas fir/western hemlock forest stands from Landsat SPOT imagery. Rem. Sens. Environ. 41, 1–17.

Cohen, W.B., Spies, T.A., Fiorella, M., 1995. Estimating the age and structure of forest in a multi-ownership landscape of western Oregon, USA. Int. J. Rem. Sens. 16, 721–746.

Cook, E.A., Iverson, L.R., Graham, R.L., 1989. Estimating forest productivity with Thematic Mapper and biogeographical data. Rem. Sens. Environ. 28, 1–17.

Curran, P.J., Dungan, J.L., Gholz, H.L., 1992. Seasonal LAI in slash pine estimated with Landsat TM. Rem. Sens. Environ. 39, 3–13.

Danson, F.M., Curran, P.J., 1993. Factors affecting the remotely sensed response of coniferous forest plantations. Rem. Sens. Environ. 43, 55–65.

De Wasseige, C., Defourny, P., 2002. Retrieval of tropical forest structure characteristics from bi-directional reflectance of SPOT images. Rem. Sens. Environ. 83, 362–375.

Drake, J.B., Dubayah, R.O., Knox, R.G., Clark, D.B., Blair, J.B., 2002. Sensitivity of large-footprint lidar to canopy structure and biomass in a neotropical rainforest. Rem. Sens. Environ. 81, 378–392.

Eastwood, J.A., Yates, M.G., Thomson, A.G., Fuller, R.M., 1997. The reliability of vegetation indices for monitoring saltmarsh vegetation cover. Int. J. Rem. Sens. 18, 3901–3907.

Eklundh, L., Harrie, L., Kuusk, A., 2001. Investigating relationships between Landsat ETM+ sensor data and leaf area index in a boreal conifer forest. Rem. Sens. Environ. 78, 239–251.

Foody, G.M., Curran, P.J., 1994. Estimation of tropical forest extent and regenerative stage using remotely sensed data. J. Biogeogr. 21, 223–244.

Franco-Lopez, H., Ek, A.R., Bauer, M.E., 2001. Estimation and mapping of forest stand density, volume, and cover type using the *k*-nearest neighbors method. Rem. Sens. Environ. 77, 251–274.

Franklin, J., 1986. Thematic Mapper analysis of coniferous forest structure and composition. Int. J. Rem. Sens. 7, 1287–1301.

Franklin, J., Hiernaux, P.H.Y., 1991. Estimating foliage and woody biomass in Sahelian and Sudanian woodlands using a remote-sensing model. Int. J. Rem. Sens. 12, 1387–1404.

Franklin, S.E., Lavigne, M.B., Deuling, M.J., Wulder, M.A., Hunt Jr., E.R., 1997. Estimation of forest leaf area index using remote-sensing and GIS data for modeling net primary production. Int. J. Rem. Sens. 18, 3459–3471.

Fransson, J.E.S., Israelsson, H., 1999. Estimation of stem volume in boreal forest using ERS-1 C- and JERS-1 L-band SAR data. Int. J. Rem. Sens. 20, 123–137.

Gemmell, F.M., 1995. Effects of forest cover, terrain, and scale on timber volume estimation with Thematic Mapper data in the rocky mountain site. Rem. Sens. Environ. 51, 291–305.

Gilabert, M.A., Conese, C., Maselli, F., 1994. An atmospheric correction method for the automatic retrieval of surface reflectance from TM images. Int. J. Rem. Sens. 15, 2065–2086.

Gong, P., Pu, R., Miller, J.R., 1995. Coniferous forest leaf area index estimation along the Oregon transect using compact airborne spectrographic imager data. Photogram. Eng. Rem. Sens. 61, 1107–1117.

Hall, F.G., Shimabukuro, Y.E., Huemmrich, K.F., 1995. Remote sensing of forest biophysical structure using mixture decomposition and geometric reflectance models. Ecol. Appl. 5, 993–1013.

Hardisky, M.A., Daiber, F.C., Roman, C.T., Klemas, V., 1984. Remote sensing of biomass and annual net aerial primary productivity of salt marsh. Rem. Sens. Environ. 16, 91–106.

Harrell, P.A., Bourgeau-Chavez, L.L., Kasischke, E.S., French, N.H.F., Christensen, N.L., 1995. Sensitivity of ERS-1 and JERS-1 radar data to biomass and stand structure in Alaskan boreal forest. Rem. Sens. Environ. 54, 247–260.

Harrell, P.A., Kasischke, E.S., Bourgeau-Chavez, L.L., Haney, E.M., Christensen Jr., N.L., 1997. Evaluation of approaches to estimating aboveground biomass in southern pine forests using SIR-C data. Rem. Sens. Environ. 59, 223–233.

Horler, D.N.H., Ahern, F.J., 1986. Forestry information content of Thematic Mapper data. Int. J. Rem. Sens. 7, 405–428.

Huete, A.R., Liu, H.Q., Batchily, K., van Leeuwen, W., 1997. A comparison of vegetation indices over a global set of TM images for EOS-MODIS. Rem. Sens. Environ. 59, 440–451.

Israelsson, H., Askne, J., Sylvander, R., 1994. Potential of SAR for forest bole volume estimation. Int. J. Rem. Sens. 15, 2809–2826.

Jakubauskas, M.K., Price, K.P., 1997. Empirical relationships between structural and spectral factors of Yellowstone lodgepole pine forest. Photogram. Eng. Rem. Sens. 63, 1375–1381.

Kimes, D.S., Holben, B.N., Nickeson, J.E., Mckee, W.A., 1996. Extracting forest ages in a pacific northwest forest from Thematic Mapper and topographic data. Rem. Sens. Environ. 56, 133–140.

Kurvonen, L., Pulliainen, J., Hallikainen, M., 1999. Retrieval of biomass in boreal forests from multitemporal ERS-1 and JERS-1 SAR data. IEEE Trans. Geosci. Rem. Sens. 37, 198–205.

Lathrop Jr., R.G., Pierce, L.L., 1991. Ground-based canopy transmittance and satellite remotely sensed measurements for estimation of coniferous forest canopy structure. Rem. Sens. Environ. 36, 179–188.

Lu, D., 2001. Estimation of forest stand parameters and application in classification and change detection of forest cover types in the Brazilian Amazon Basin, Ph.D. Dissertation, Indiana State University.

Lu, D., Mausel, P., Brondizio, E., Moran, E., 2002a. Aboveground biomass estimation of successional and mature forests using TM images in the Amazon Basin. In: D. Richardson, P. van Oosterom (Eds.), Advances in Spatial Data Handling, Springer-Verlag, New York, pp. 183–196.

Lu, D., Mausel, P., Brondizio, E., Moran, E., 2002b. Assessment of atmospheric correction methods for Landsat TM data applicable to Amazon basin LBA research. Int. J. Rem. Sens. 23, 2651–2671.

Lucas, R.M., Honzák, M., Foody, G.M., Curran, P.J., Corves, C., 1993. Characterizing tropical secondary forests using multi-temporal Landsat sensor imagery. Int. J. Rem. Sens. 14, 3061–3067.

Markham, B.L., Barker, J.L., 1987. Thematic Mapper bandpass solar exoatmospheric irradiances. Int. J. Rem. Sens. 8, 517–523.

McDonald, A.J., Gemmell, F.M., Lewis, P.E., 1998. Investigation of the utility of spectral vegetation indices for determining information on coniferous forests. Rem. Sens. Environ. 66, 250–272.

Moran, E.F., 1981. Developing the Amazon. Indiana University Press, Bloomington, Ind.

Moran, E., Brondizio, E.S., McCracken, S., 2002. Trajectories of land use: soils, succession, and crop choice. In: C. Wood, R. Porro (Eds.), Deforestation and Land Use in the Amazon. University of Florida Press, Gainesville, pp. 193–217.

Nelson, B.W., Mesquita, R., Pereira, J.L.G., de Souza, S.G.A., Batista, G.T., Couto, L.B., 1999. Allometric regression for improved estimate of secondary forest biomass in the central Amazon. For. Ecol. Manage. 117, 149–167.

Nelson, R.F., Kimes, D.S., Salas, W.A., Routhier, M., 2000. Secondary forest age and tropical forest biomass estimation using Thematic Mapper Imagery. BioScience 50, 419–431.

Nemani, R., Pierce, L., Running, S., Band, L., 1993. Forest ecosystem processes at the watershed scale: sensitivity to remotely sensed leaf area index estimated. Int. J. Rem. Sens. 14, 2519–2534.

Overman, J.P.M., Witte, H.J.L., Saldarriaga, J.G., 1994. Evaluation of regression models for above-ground biomass determination in Amazon rainforest. J. Trop. Ecol. 10, 207–218.

Peterson, D.L., Spanner, M.A., Running, S.W., Teuber, K.B., 1987. Relationship of Thematic Mapper simulator data to leaf area index of temperate coniferous forests. Rem. Sens. Environ. 22, 323–331.

Peterson, D.L., Westman, W.E., Stephenson, N.J., Ambrosia, V.G., Brass, J.A., Spanner, M.A., 1986. Analysis of forest structure using Thematic Mapper simulator data. IEEE Trans. Geosci. Rem. Sens. 24, 113–121.

Rauste, J., Hame, T., 1994. Radar-based forest biomass estimation. Int. J. Rem. Sens. 15, 2797–2808.

Ripple, W.J., Wang, S., Isaacson, D.L., Pairre, D.P., 1991. A preliminary comparison of Landsat Thematic Mapper and SPOT-1 HRV multispectral data for estimating coniferous forest volume. Int. J. Rem. Sens. 12, 1971–1991.

Roy, P.S., Ravan, S.A., 1996. Biomass estimation using satellite remote-sensing data – an investigation on possible approaches for natural forest. J. Biosci. 21, 535–561.

Sader, S.A., Waide, R.B., Lawrence, W.T., Joyce, A.T., 1989. Tropical forest biomass and successional age class relationships to a vegetation index derived from Landsat TM data. Rem. Sens. Environ. 28, 143–156.

Santoro, M., Askne, J., Smith, G., Fransson, J., 2001. Stem volume retrieval in boreal forests from ERS-1/2 interferometry. Rem. Sens. Environ. 81, 19–35.

Santos, J.R., Pardi Lacruz, M.S., Araujo, L.S., Keil, M., 2002. Savanna and tropical rainforest biomass estimation and spatialization using JERS-1 data. Int. J. Rem. Sens. 23, 1217–1229.

Song, C., Woodcock, C.E., Seto, K.C., Lenney, M.P., Macomber, S.A., 2001. Classification and change detection using Landsat TM data: when and how to correct atmospheric effect? Rem. Sens. Environ. 75, 230–244.

Spanner, M.A., Pierce, L.L., Peterson, D.L., Running, S.W., 1990. Remote sensing of temperate coniferous leaf area index: the influence of canopy closure, understory vegetation, and background reflectance. Int. J. Rem. Sens. 11, 95–111.

Stefan, S., Itten, K.I., 1997. A physically based model to correct atmospheric and illumination effects in optical satellite data of rugged terrain. IEEE Trans. Geosci. Rem. Sens. 35, 708–717.

Steininger, M.K., 2000. Satellite estimation of tropical secondary forest above-ground biomass: data from Brazil and Bolivia. Int. J. Rem. Sens. 21, 1139–1157.

Stenback, J.M., Congalton, R.G., 1990. Using Thematic Mapper imagery to estimate forest understory. Photogram. Eng. Rem. Sens. 56, 1285–1290.

Sun, G., Ranson, K.J., Kharuk, V.I., 2002. Radiometric slope correction for forest biomass estimation from SAR data in the western Sayani Mountains, Siberia. Rem. Sens. Environ. 79, 279–287.

Tetuko, J., Tateishi, R., Wikantika, K., 2001. A method to estimate tree trunk diameter and its application to discriminate Java-Indonesia tropical forests. Int. J. Rem. Sens. 22, 177–183.

Treitz, P.M., Howarth, P.J., 1999. Hyperspectral remote-sensing for estimating biophysical parameters of forest ecosystems. Prog. Phys. Geogr. 23, 359–390.

Trotter, C.M., Dymond, J.R., Goulding, C.J., 1997. Estimation of timber volume in a coniferous plantation forest using Landsat TM. Int. J. Rem. Sens. 18, 2209–2223.

Tucker, C.J., Vanpraet, C.L., Boerwinkle, E., Gaston, A., 1983. Satellite remote-sensing of total dry matter accumulation in the Senegalese Sahel. Rem. Sens. Environ. 13, 461–474.

Tucker, J.M., Brondízio, E.S., Moran, E.F., 1998. Rates of forest regrowth in Eastern Amazonia: a comparison of Altamira and Bragantina regions, Pará State, Brazil. Interciencia 23, 64–73.

Turner, D.P., Cohen, W.B., Kennedy, R.E., Fassnacht, K.S., Briggs, J.M., 1999. Relationships between leaf area index and Landsat TM spectral vegetation indices across three temperate zone sites. Rem. Sens. Environ. 70, 52–68.

Vermote, E., Tanre, D., Deuze, J.L., Herman, M., Morcrette, J.J., 1997. Second simulation of the satellite signal in the solar spectrum, 6S: an overview. IEEE Trans. Geosci. Rem. Sens. 35, 675–686.

Vygodskaya, N.N., Gorshkova, I.I., Fadeyeva, Y.V., 1989. Theoretical estimates of sensitivity in some vegetation indices to

variation in the canopy condition. Int. J. Rem. Sens. 10, 1857–1872.

Wu, S., 1990. Assessment of tropical forest stand characteristics with multipolarisation SAR data acquired over a mountainous region in Costa Rica. IEEE Trans. Geosci. Rem. Sens. 28, 752–755.

Wulder, M., 1998. Optical remote-sensing techniques for the assessment of forest inventory and biophysical parameters. Prog. Phys. Geogr. 22, 449–476.

Wulf, R.R.D., Goossens, R.E., Roover, D.P.D., Borry, F.C., 1990. Extraction of forest stand parameters from panchromatic and multispectral SPOT-1 data. Int. J. Rem. Sens. 11, 1571–1588.